ARMA 10-171

Inverting for creep strain parameters of uncemented reservoir sands using arbitrary stress-strain data

Hagin, P.N.
Chevron ETC, San Ramon, California, USA
Zoback, M.D.
Stanford University, Stanford, California, USA

This paper was prepared for presentation at the 44th US Rock Mechanics Symposium and 5th U.S.-Canada Rock Mechanics Symposium, held in Salt Lake City, UT June 27–30, 2010.

ABSTRACT: Creep strain experiments on uncemented reservoir sands suggest that the time-dependent component of deformation can be modeled using linear viscoelasticity theory. The standard approach to solving for the values of the appropriate model parameters is to fit creep strain data as a function of time. However, by writing the creep compliance function in terms of strain-rate rather than strain, it is possible to solve for the values of the model parameters using arbitrary time-histories of stress-strain data. Rewriting the creep compliance function as the conjugate stress relaxation function allows constant loading-rate or step-hold loading data to be used to constrain the model. Complex loading histories can be divided into branches of approximately constant stress- or strain-rate and solved piecewise. After deriving the necessary equations, we show that the method successfully reproduces the known creep compliance function of an example uncemented reservoir sand.

1. INTRODUCTION

Producing oil and gas from uncemented sand reservoirs is often accompanied by a host of interesting challenges. As these formations can be weak and prone to sand-production [e.g. 1], unique approaches to drilling and completions may be required to minimize the risk of excessively damaging wells. Uncemented sand reservoirs are also associated with significant time-dependent compaction, as observed in numerous fields around the world using 4-D seismic monitoring [2-5], and documented in the laboratory [6-8]. Reservoir compaction can be beneficial if it provides pressure support by mechanically squeezing reservoir fluids as porosity is being lost (so-called compaction drive). On the other hand, the compaction-induced loss of porosity can also cause a dramatic loss in formation permeability [9, 10]. Given the potential complications associated with production in uncemented sands, a model capable of predicting the compaction associated with changes in reservoir pressure is desirable.

In previous work, we showed that linear viscoelasticy theory could be used to model the time-dependent compaction of uncemented sand reservoirs from California and the Gulf of Mexico [11]. In the laboratory, time-dependent deformation is most often observed and characterized by conducting creep-strain experiments [e.g. 12]. However, creep-strain data are not routinely collected or reported in the literature, so it would be useful to have a means for obtaining creep function parameters from whatever data is available. In this paper we construct a relatively simple method for deriving creep function parameters from arbitrary data sets using linear viscoelasticity as a framework.

2. BACKGROUND

The mathematical framework for linear viscoelasticity theory has been extensively written about in the mechanical and biomedical engineering literature. Lakes [13] provides an excellent overview of both theoretical and experimental methods; an exhaustive treatment of linear viscoelastic constitutive models can be found in Tschoegl [14]. A robust and generic inverse method to solve for creep function parameters using dynamic frequency-domain measurements was introduced by Baumgaertel and Winter [15]. Their methodology has since been extended to take into account time-domain data [16], simplified experimental procedures [17], and different stress paths [18]. Park *et al* [18] derive a 3-D viscoelastic constitutive law for asphalt that includes the effects of damage. While this level of mathematical complexity indicates the maturity of the theory, in this paper we will make a number of simplifying assumptions, based on previous laboratory observations.

In general, linear phenomenological (spring and dashpot) models fail to capture the behavior of viscoelastic materials [13]. However, previous studies on uncemented sands suggest that creep strain can be described using an analytical power law function [11,12]. Furthermore, Chang *et al* [19] found that creep strain data collected under hydrostatic, triaxial, and uniaxial strain boundary conditions could all be accurately modeled using the same function, implying that a full 3-D representation using tensors is not necessary. So, for the purpose of this study, we will assume that the deformation of uncemented sands can be described using 1-D, phenomenological, linear viscoelastic models.

3. INVERTING FOR CREEP FUNCTION PARAMETERS – THEORY

In the context of this study, only two key aspects of linear viscoelasticity theory are needed: linearity, which requires the strain at a given time to be a linear function of stress, and superposition, which requires the strain response of a compound loading history to equal the sum of the strain responses to the individual components of that loading history. In combination, this means that the strain response to any time-series of stresses can be found if the impulse or step function response is known.

Recall that creep strain accumulates as a function of time in response to a step increase in stress, $\varepsilon(t) = \sigma_0 J(t)$, where $\varepsilon(t)$ is creep strain, σ_0 is the stress magnitude of a Heaviside step function (H(t)), and J(t) is the creep compliance function. Once J(t) is known, the strain response to any arbitrary loading history can be found using superposition. Figure 1 shows a simple creep strain example composed of a positive step in stress followed by a larger negative step, such that the sum of the stresses is zero. The stress history can be written as the superposition of a step up followed by a step down, as shown in Figure 2,

$$\sigma(t) = \sigma_0\left[\mathrm{H}(t) - \mathrm{H}(t - t_1)\right] \qquad (1)$$

and the resulting strain follows from Boltzmann superposition theory, as shown in Figure 3,

$$\varepsilon(t) = \sigma_0\left[J(t) - J(t - t_1)\right]. \qquad (2)$$

To generalize the proceeding example to any arbitrary stress history, the single value of t_1 in Equations 1 and 2 may simply be replaced with a variable, τ. The example shown in Figure 1 can now be written as follows:

$$\sigma(t) = \sigma(\tau)\left[\mathrm{H}(t - \tau) - \mathrm{H}(t - \tau + \Delta\tau)\right]. \qquad (3)$$

By once again exploiting the superposition principle, the associated strain history as a function of time is given by Equation 4, and shown in Figure 4,

$$\varepsilon(t) = \sigma(\tau)\left[J(t - \tau) - J(t - \tau + \Delta\tau)\right]. \qquad (4)$$

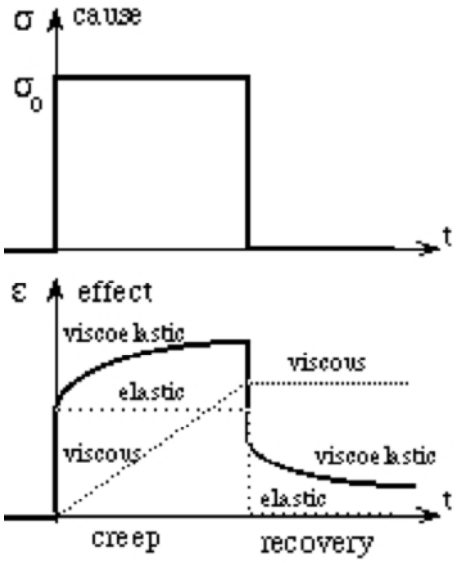

Figure 1: Creep strain and recovery response of a linear viscoelastic material caused by a boxcar stress function. The strain response can be constructed using Boltzmann superposition. Unmodified from [13].

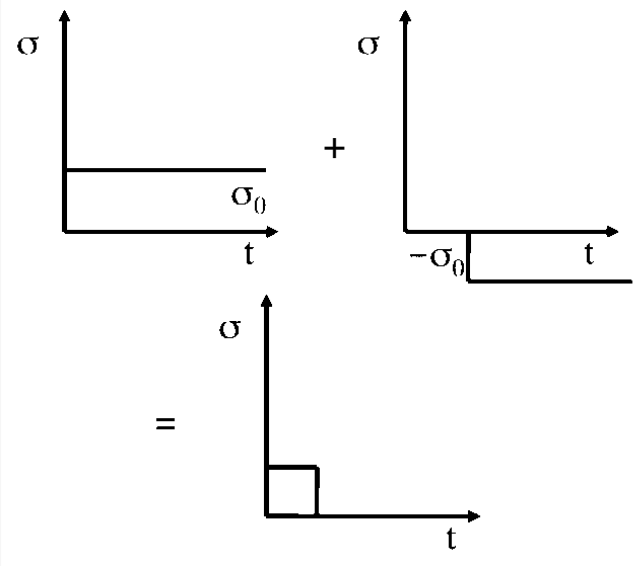

Figure 2: Graphical representation of the boxcar stress function described by Equation 1.

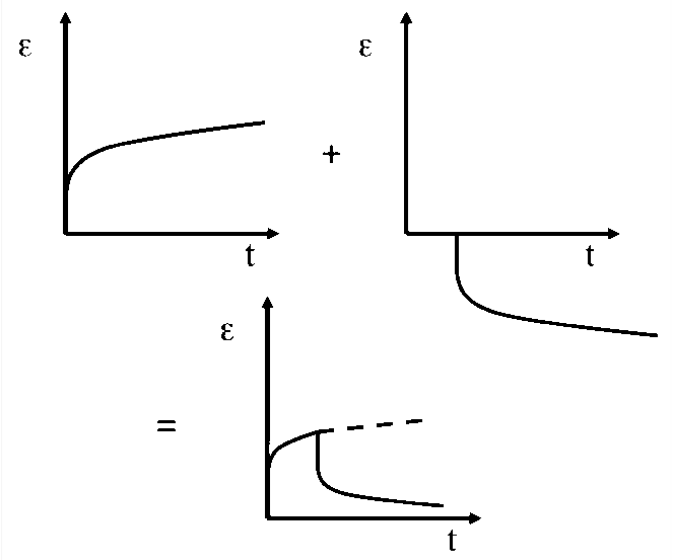

Figure 3: Graphical representation of the linear viscoelastic strain response to the boxcar stress function shown in Figure 2, as described by Equation 2.

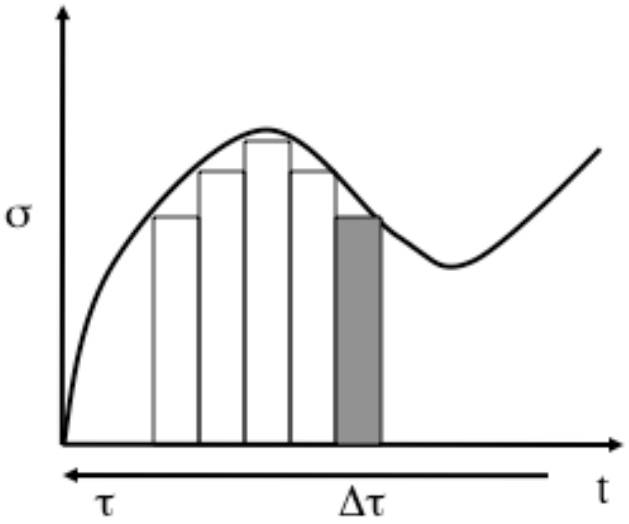

Figure 4: Graphical representation of Equation 4, showing how an arbitrary stress history can be constructed using a series of boxcar functions.

Taking the limit as Δt goes to zero gives the strain response to an impulse function of stress:

$$d\varepsilon(t) = -\sigma(\tau)\frac{dJ(t-\tau)}{d\tau}. \qquad (5)$$

Any stress history can be broken up into a series of impulse functions, and the corresponding strain at time *t* can be found by summing or integrating the effects of each preceding stress pulse. Integrating Equation 5 by parts, to shift the derivative from the creep function to the stress function, results in the following relationship between stress and strain as a function of time:

$$\varepsilon(t) = \int_0^t J(t-\tau)\frac{d\sigma(\tau)}{d\tau}\,d\tau, \qquad (6)$$

where the only requirement is that the stress history needs to be a piecewise continuous and differentiable function of time.

Common experimental protocols call for either step increases in stress followed by creep holds, or continuous loading at a constant rate. Using the Boltzmann superposition principle and the Equations from the previous paragraph, deriving the strain response to a constant stress rate is fairly straightforward. Assuming that the material is subjected to a constant stress rate (S) starting a time zero, and introducing *T* as an integration variable, results in the following relationship between stress rate and strain:

$$\varepsilon(t) = \int_0^t J(t-\tau)\frac{d\sigma(\tau)}{d\tau}\,d\tau = \int_0^t J(t-\tau)S\,d\tau = -S\int_0^t J(T)\,dT. \qquad (7)$$

By applying Liebnitz' rule [13], Equation 7 can be simplified to relate stress rate and strain rate:

$$\frac{d\varepsilon(t)}{dt} = SJ(t). \qquad (8)$$

The stress-strain type-curve associated with Equation 8 is illustrated in Figure 5 for several stress rates.

Because creep strain can also be written in terms of strain rate decay, it is possible to solve for J(t) using data consisting of constant stress rate loading and creep holds. For this study, a power law function of creep is assumed, of the form $J(t) = J_0 + At^n$, but in practice, any piece-wise continuous integrable function can be used [15].

Figure 5: Graphical representation of Equation 8, showing the effect of increasing stress rate on the resulting stress-strain curve of a linear viscoelastic material. Apparent stiffness increases with stress rate.

4. INVERTING FOR CREEP FUNCTION PARAMETERS – EXAMPLE

Having derived the necessary equations to solve for the parameters of a creep compliance function (of arbitrary form) using stress-strain data from a constant stress or strain rate test, we will now demonstrate the validity of the method using laboratory data from an experiment performed on an uncemented reservoir sand from the Wilmington field, offshore California. Wilmington sand was selected because the creep compliance function is already known, from prior work [11].

4.1. Sample Description and Experimental Background

Core samples of uncemented sand were obtained Wilmington field at a depth of approximately 1 kilometer. Because the sand is part of a turbidite sequence, mineralogy is mixed, including 30% quartz, 30% potassium feldspar, 15% smectite, and lesser amounts of micas and lithic fragments. Grain angularity is highly variable, porosity is approximately 30%, and permeability is on the order of 100 mD.

In order to test the inversion method described in Section 3, we need to perform a constant stress or strain rate test on an uncemented sand with a known creep compliance function. Our prior experimental work on Wilmington sand investigated creep strain, and we found a model that successfully predicted long-term compaction in the reservoir [11]. This model decoupled the total deformation into instantaneous and time-dependent parts, which were described by power law functions of stress and time, respectively. The model and example data used to derive the fitting parameters are shown in Figures 6 and 7. Note that these tests were performed on room-dry samples, in an effort to eliminate time-dependent pressure diffusion or fluid drainage effects. Pore volume strain and bulk volume strain are related using the poroelasticity equations of Zimmerman [20].

4.2. Modeling Results

The laboratory data used to the test the creep function inversion method described in Section 3 are shown in Figure 8. The figure shows the stress-strain curve produced by hydrostatically loading a sample under constant volumetric strain rate boundary conditions. This sample was loaded at a strain rate of 10^{-4}/s, in an effort to physically decouple the instantaneous and time-dependent components of deformation. These hydrostatic stress and volumetric strain data are used to invert for the best-fitting creep function parameters. The solution produces the predicted strain curve shown in red in Figure 9.

The red curve in Figure 9 shows the application of Equation 7 derived for the case of a constant volumetric strain rate. In this case, we solve directly for the parameters of the stress relaxation function, and then invert the equation to find the corresponding creep compliance function parameters (for reference see [13]).

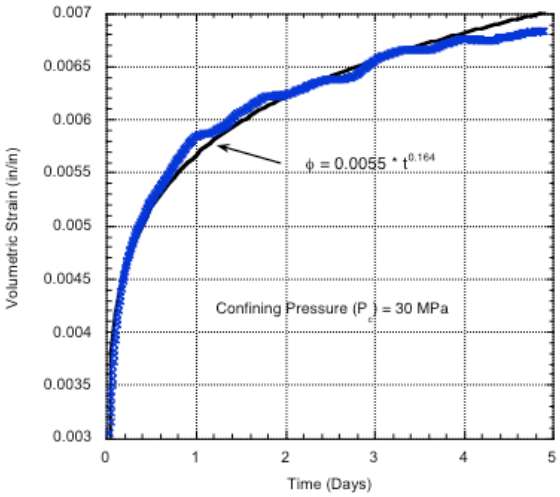

Figure 6: Volumetric strain as a function of time in days for a room-dry Wilmington sand sample. This is the creep strain data resulting from an ideal creep strain test, in which the sample is instantaneously loaded from 0 to 30 MPa. The creep strain data is modeled using a power law function of time, as shown by the black line.

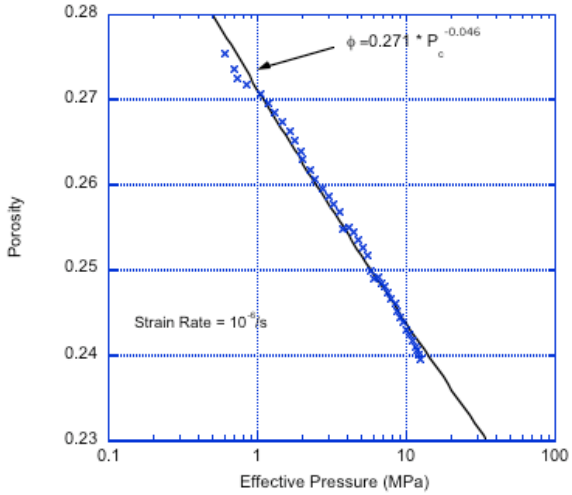

Figure 7: Porosity plotted as a function of effective hydrostatic stress (pressure) for a room-dry Wilmington sand sample. Note that this is a semi-log plot. For this test, the sample was loaded under constant volumetric strain rate boundary conditions, at a strain rate of 10^{-6}/s. These data are used to model the instantaneous component of deformation, in this case with a power law function.

The black curve in Figure 9 shows the best-fitting power-law function that relates stress to instantaneous strain. Note that this is the same function shown in Figure 7. Note that the strain data starts to deviate from the curve at approximately 20 MPa, which is the maximum *in situ* stress the sample has experienced. Above this threshold stress, we observe the onset of viscous time-dependent and rate-dependent deformation. To apply Equation 7, the instantaneous component of

deformation is subtracted from the total strain, and time prior to the onset of viscous deformation is subtracted from the total time. In other words, the data are normalized in strain and time to make it easier to apply the model.

Figure 10 shows the validity of the method, as the parameters of the creep compliance function derived from fitting the constant strain-rate data reproduce those derived from fitting the ideal creep strain data shown in Figure 6. The difference is less than 1% for the amplitude, and 2.5% for the time constant of the power law creep function. These differences could represent error in the method, or could reflect real differences in the behavior of the samples, as the Wilmington sand is part of a turbidite sequence, and hence very heterogeneous.

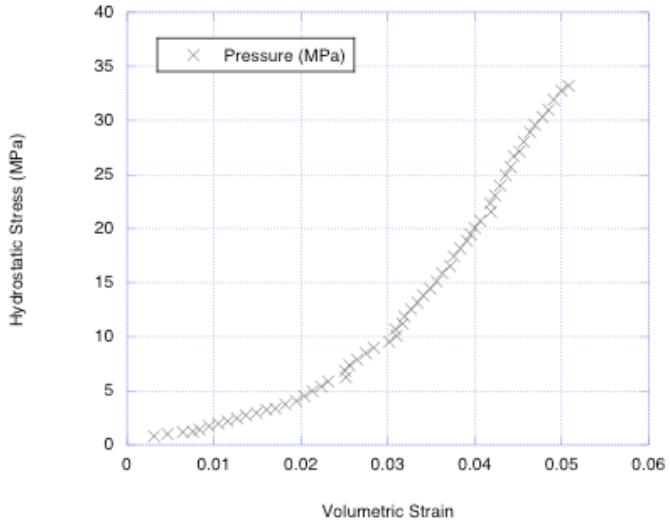

Figure 8: Effective hydrostatic stress plotted as a function of volumetric strain for a room-dry Wilmington sand sample. For this test, the sample was loaded under constant volumetric strain rate boundary conditions, at a strain rate of 10^{-4}/s.

5. DISCUSSION

While the mathematics presented here only describe the behavior of ideal linear viscoelastic materials, the framework can be generalized. It is difficult but possible to extend the equations to include nonlinear effects; the creep function could be written as $J(\sigma,t) = \sigma^m(J_0 + At^n)$ in which case strain becomes a power function of both stress and time. While the Equations were all written in terms of scalars, and deformation was assumed to be isotropic, writing the relationships in terms of tensors and three-dimensions is possible. Doing this would allow for anisotropy as well as the effects of different boundary conditions, although many more tests would be required to constrain all of the model parameters. Finally, while the effects of pore fluids were not discussed here, by assuming that the fluid is non-reactive, and can be described by one-dimensional diffusion, it is possible to include the effects of fluid expulsion and imbibition in a separate, quasi-creep function.

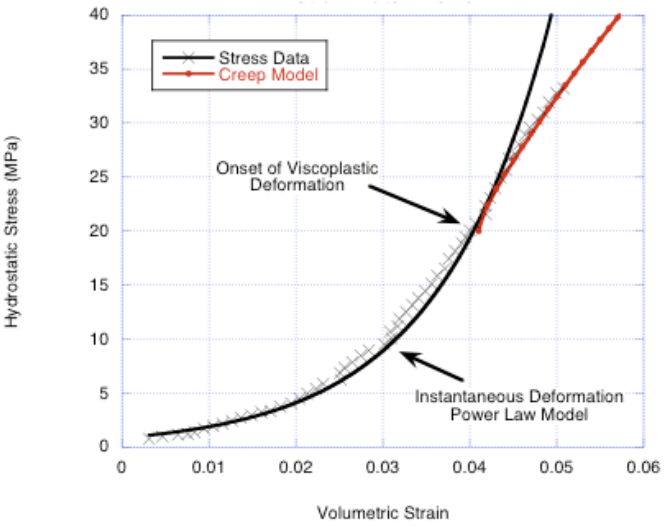

Figure 9: Same data as shown in Figure 8, with modeling results. The black line shows the predicted instantaneous deformation, using the model parameters from Figure 7. The red line shows the predicted time-dependent component of deformation after inverting the data for creep compliance function values using the method described in Section 3.

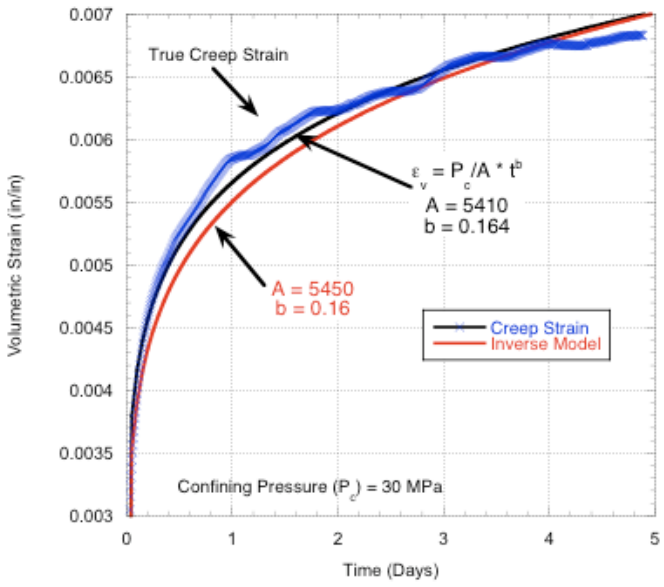

Figure 10: Ideal creep strain curve from Figure 6 comparing the original best-fitting power law model with the model parameters derived by inverting the constant strain-rate data shown in Figures 8 and 9.

6. CONCLUSIONS

Significant time-dependent compaction is commonly observed in unconsolidated sand reservoirs. It would be useful to predict the magnitude and spatial extent of this compaction prior to production. However, experimental creep strain data are not always available for analysis and to provide constraints for modeling. In this paper we

derive equations using linear viscoelasticity theory so that creep functions can be obtained from any available laboratory data. Creep strain experiments are not required. Instead, any arbitrary loading history, under any boundary conditions, can be used to invert for the creep function parameter values.

REFERENCES

1. Han, G., M.B. Dusseault, and J. Cook, 2002. Quantifying Rock Capillary Strength Behavior in Unconsolidated Sandstones, SPE/ISRM 78170. Presented at the *SPE/ISRM Rock Mechanics Conference, Irving, Texas, 20-23 October, 2002.*
2. Guilbot, J., and B. Smith, 2002, 4D constrained depth conversion for reservoir compaction estimation: Application to Ekofisk field. *The Leading Edge*, 21: 302–308.
3. Hatchell, P., and S. Bourne, 2005, Rocks under strain: Strain-induced time-lapse time shifts are observed for depleting reservoirs. *The Leading Edge*, 24: 1222–1225.
4. Hatchell, P., A. van den Beukel, M. Molenaar, K. Maron, C. Kenter, J. Stammeijer, J. van der Velde, and C. Sayers, 2003, Whole earth 4D: Reservoir monitoring geomechanics: *73rd Annual International Meeting, SEG, Expanded Abstracts*, 1222–1225.
5. Landro, M., 2001, Discrimination between pressure and fluid saturation changes from time-lapse seismic data *Geophysics*, 66: 836–844.
6. Ostermeier, R. M., 1995, Deepwater Gulf of Mexico turbidites — compaction effects on porosity and permeability, *SPE Formation Evaluation*, 10: 79–85.
7. de Waal, J. A., and R. M. Smits, 1988, Prediction of reservoir compaction and surface subsidence: Field application of a new model, *SPE Formation Evaluation*, 3: 347–356.
8. Hagin, P. N., and M. D. Zoback, 2004a, Viscous deformation of unconsolidated sands — Part I: Time-dependent deformation, frequency dispersion, and attenuation, *Geophysics*, 69: 731–741.
9. Chan, A., P. N. Hagin, and M. D. Zoback, 2004, Viscoplastic deformation, stress and strain paths in unconsolidated sands part 2: Field applications using dynamic DARS, *Society of Petroleum Engineers/ American Rock Mechanics Society Paper 04-568*.
10. Yale, D.P., and B. Crawford, 1998. Plasticity and Permeability in Carbonates: Dependence on Stress Path and Porosity. SPE 47582. In the Proceedings of the *SPE/ISRM Rock Mechanics in Petroleum Engineering, 8-10 July 1998, Trondheim, Norway*.
11. Hagin, P. N., and M. D. Zoback, 2007, Predicting and monitoring long-term compaction in unconsolidated reservoir sands using a dual power law model, *Geophysics*, 72: 165-173.
12. Dudley, J., M. Myers, R. Shew, and M. Arasteh, 1994, Measuring compaction and compressibilities in unconsolidated reservoir materials via time-scaling creep, In the proceedings of the *Eurock International Meeting, International Society of Rock Mechanics*, 45–54.
13. Lakes, R., 1999, *Viscoelastic Solids*, CRC Press, Boca Raton, Florida.
14. Tschoegl, N. W., 1989, *The Phenomenological Theory of Linear Viscoelastic Behavior*, Springer Verlag, Berlin.
15. Baumgaertel, M., and H. H. Winter, 1989, Determination of discrete relaxation and retardation time spectra from dynamic mechanical data, *Rheologica Acta*, 28: 511-519.
16. Kaschta, J., and F.R. Schwarzl, 1994, Calculation of discrete retardation spectra from creep data 1 – Method, *Rheologica Acta*, 33: 517-529.
17. Nikonov, A., Davies, A. R., and I. Emri, 2005, The determination of creep and relaxation functions from a single experiment, *Journal of Rheology*, 49 (6): 1193-1211.
18. Park, S. W., Kim, R. Y., and R. A. Schapery, 1996, A viscoelastic continuum damage model and its application to uniaxial behavior of asphalt concrete, *Mechanics of Materials*, 24: 241-255.
19. Chang, C., D. Moos, and M. D. Zoback, 1997, Anelasticity and dispersion in dry unconsolidated sands, *International Journal of Rock Mechanics*, 34, 402-405.
20. Zimmerman, R., W. Somerton, and M. King, 1986, Compressibility of Porous Rocks, *Journal of Geophysical Research*, 91(B12), 12765-12777.